International Journal of Mechanical and Materials Engineering (IJMME), Vol. 3 (2008), No.2, 198-205.

DRAG CO-EFFICIENT IN A CRYSTAL SUSPENSION

N. M. S. Hassan[1], M. M. K. Khan[2], M. G. Rasul[2] and D.W. Rackemann[3]
[1]Process Engineering & Light Metals (PELM) Centre, Faculty of Sciences, Engineering and Health
CQUniversity, Rockhampton, Queensland, 4702, AUSTRALIA
[2]College of Engineering and Built Environment, Faculty of Sciences, Engineering and Health
CQUniversity, Rockhampton, Queensland, 4702, AUSTRALIA
[3]Sugar Research and Innovation
Queensland University of Technology, Brisbane, Queensland, 4001, AUSTRALIA
Email: n.hassan@cqu.edu.au, nmshassan@gmail.com

ABSTRACT

A single air bubble rising in xanthan gum crystal suspension has been studied experimentally. The suspension was made by different concentrations of xanthan gum solutions with 0.23 mm polystyrene crystal particles. Drag co-efficient data and a new correlation of drag coefficient is presented for spherical and non-spherical bubbles in non-Newtonian crystal suspension. The correlation is developed in terms of the Reynolds number, Re and the bubble shape factor, ϕ (the ratio between the surface equivalent sphere diameter to the volume equivalent sphere diameter). The experimental drag coefficient was found to be consistent with this new predicted correlation and published data over the ranges, $0.1<\mathrm{Re}<200$ and $1<\phi<2.5$.

Key words: Crystal suspension, bubble rise velocity, drag co-efficient, bubble shape factor

INTRODUCTION

The terminal velocity and drag co-efficient of an air bubble are dependent on the properties of the liquid as well as the bubble. The terminal velocity of an air bubble is defined as the velocity attained at steady state conditions where all applied forces are balanced. The drag co-efficient correlates the drag force exerted on a moving air bubble to its terminal velocity and projected surface area. The knowledge or prediction of terminal velocity and drag co-efficient are significant characteristics that are required for application to multiphase engineering problems. There are many empirical and semi-empirical correlations of the drag co-efficient existing in literature which are applicable over either a limited or wide range of Reynolds numbers (Re). Clift *et al.* (2005) have listed many empirical or semi-empirical correlations to predict the drag curves of rising or falling bubbles or particles for the wide range of Re. Most of these correlations are based on spherical bubbles or particles. A number of correlations were proposed for non-spherical particles by Haider & Levenspiel (1989) and Thompson & Clark (1991), Haider & Levenspiel (1989) and Tran-Cong *et al.* (2004) generally used the volume equivalent sphere diameter and sphericity factor for the prediction of the drag co-efficient. Other researchers (Thompson & Clark, 1991; Madhav & Chhabra, 1995) introduced a shape factor for the determination of drag co-efficient of non-spherical particles. For the non-Newtonian power-law fluid, the calculation of drag co-efficient exhibited an additional dependence on the power law index (n) (Dalton, 1967; Prakash, 1983; Kelessidis, 2004). Investigations by Dhole *et al.* (2007) found that the drag co-efficient always increased with an increase in 'n' for all Re. Some researchers disagreed with this finding (Lali *et al,* 1989). Later, Chhabra (1990a, 2006b) reported that the Newtonian standard drag curves also provided an adequate demonstration of the $C_d - \mathrm{Re}$ data for power law fluids. Many investigators (Chhabra, 1990a & 2006b; Kelessidis, 2004) suggested that the $C_d - \mathrm{Re}$ correlations for Newtonian fluids could be extended to non-Newtonian fluids, if Re was calculated on the basis of the apparent viscosity of the liquid. Recently, Shah *et al.* (2007) predicted a new model for the terminal velocity of a spherical particle rising in inelastic power law fluids. The new model for terminal velocity gave a closer prediction to the experimental data compared to the widely used Newtonian standard drag curves.

Karamanev (1994) presented a semi-analytical equation which explained how the internal circulation of the bubble has no effect on the terminal rise velocity and that the bubble drag co-efficient could be computed on the basis of its real shape. For the case of power-law non-Newtonian fluids, it has been shown that the drag curve for air bubbles followed Hadamard-Rybczynski model rather than Stokes model for Re < 5 (Dewsbury *et al,* 2000). On the other hand, Miyahara & Yamanaka (1993) reported for the case of highly viscous non-Newtonian liquid that the drag co-efficient deviates from the Hadamard – Rybczynski type equation if the Re increases. Dewsbury *et al.* (2000) determined experimentally that the drag co-efficient for a rising solid

sphere in non-Newtonian pseudo plastic liquids were significantly affected by its trajectory. A new drag correlation for rising spheres in power-law liquids was presented by Dewsbury *et al.* (2002). It is valid for 0.1<Re<25000. It describes the relationship between C_d and Re in creeping, transitional and turbulent flow regimes. Margaritis *et al.* (1999) studied the drag co-efficient variation for bubbles over a wide range of Re in different non-Newtonian polysaccharide solutions and proposed a correlation which matched well with experimental data.

All aforementioned studies, in general, dealt with either the drag co-efficient correlation for spherical bubbles or non-spherical particles in Newtonian and non-Newtonian power law fluids. There is no literature available on the correlation of the drag co-efficient for non-spherical bubbles in non-Newtonian crystal suspensions. This study investigated the behaviour of the drag relationship in non-Newtonian crystal suspension. A new drag correlation is proposed and compared with the results of other analytical and experimental studies available in the literature.

THEORETICAL CONSIDERATION

Bubbles achieve their terminal velocity when the forces acting on the bubble are balanced, resulting in zero acceleration. Mathematically, a bubble asymptotically approaches and can never reach its terminal velocity. The forces acting on a rising bubble are mainly, gravity (F_G), buoyancy (F_B) and drag (F_D) and the magnitude of these forces is dependent on the bubble and fluid properties and their mathematical explanation is given by,

Gravity force:

$$F_G = V \rho_{air} g \tag{1}$$

where: V = bubble volume (m^3); ρ_{air} = air bubble density (kg/m^3); g = gravity (m/s^2)

Buoyancy force:

$$F_B = V \rho_{liq} g \tag{2}$$

where: ρ_{liq} = liquid density (kg/m^3)

Drag force:

An expression for the drag force on a bubble is usually given in the form,

$$F_D = C_d A \rho_{liq} \left(\frac{U_b^2}{2} \right) \tag{3}$$

where: C_d = drag co-efficient; F_D = drag force, A = projected surface area (m^2); U_b = bubble rise or terminal velocity (m/s).

At steady state terminal velocity, the balance of the forces is given by,

$$F_D = \left| F_B - F_G \right| \tag{4}$$

Substituting equations (1), (2) and (3) into equation (4) yields,

$$C_d A \rho_{liq} \left(\frac{U_b^2}{2} \right) = V \left| \rho_{air} - \rho_{liq} \right| g \tag{5}$$

$$\text{And } C_d A \rho_{liq} \left(\frac{U_b^2}{2} \right) = V \Delta \rho g \tag{6}$$

Using a spherical geometry, the volume-equivalent sphere diameter was introduced by Wadel (1933) which is defined as, $d_{eq} = \sqrt[3]{\frac{6V}{\pi}}$ or $V = \left(\frac{\pi}{6} \right) d_{eq}^3$, where V is the bubble volume and d_{eq} is the bubble equivalent diameter. Again, the projected surface area of the bubble is also delineated as $A = \left(\frac{\pi}{4} \right) d_w^2$ or $d_w = \sqrt{\frac{4A}{\pi}}$ where d_w is bubble characteristics diameter or long axis diameter of the bubble. The drag co-efficient at steady state conditions for non-spherical bubble is calculated by rearranging equation (6):

$$C_d = \frac{4 g d_{eq}^3 \Delta \rho}{3 d_w^2 \rho_{liq} U_b^2} \tag{7}$$

For the case of spherical bubble, equation (6) can be reduced as follows:

$$C_d = \frac{4 g d_w \Delta \rho}{3 \rho_{liq} U_b^2} \tag{8}$$

The ratio of $\frac{d_w}{d_{eq}}$ is an important dimensionless number which was used in many studies (Khan & Richardson, 1987; Unnikrishan & Chhabra, 1991) for the calculation of drag co-efficient of non-spherical particles or bubbles. It was commonly distinguished that C_d must be articulated in terms of Re and shape factors for non-spherical particles or bubbles in any medium. Several methods were introduced for obtaining these shape factors which were used to classify the non-spherical bubbles or particles (Clift *et al,* 2005). The shape factor(ϕ) is a widely used method for attaining the bubble or particle shape. ϕ is defined (Haider & Levenspiel, 989; Wadel , 1993; Gabito & Tsouris, 2008) as,

$$\phi = \frac{A}{A_V} = \frac{6d_w^2}{4d_{eq}^3} \quad \therefore \phi = \frac{d_w}{d_{eq}} = \frac{\sqrt{4A}}{\sqrt[3]{6A_V}} \tag{9}$$

Where, A_V is the surface of a sphere having the same volume as the bubble which is equal to $\left(\frac{\pi}{6}\right)d_{eq}^3$.

Thus, equation (7) can be written as,

$$C_d = \frac{2g\Delta\rho}{\phi\rho_{liq}U_b^2} \tag{10}$$

Again, equation (10) can be arranged by,

$$C_d = \frac{K_1}{\phi U_b^2} \text{ or } C_d = K_1\left(\frac{1}{\phi U_b^2}\right) \tag{11}$$

It is assumed that $K_1 = \frac{2g\Delta\rho}{\rho_{liq}}$ is constant for any particular gas-liquid system but $\frac{1}{\phi}$ and $\frac{1}{U^2}$ vary with the change of bubble size. Hence, the value of C_d is dependent on ϕ and U_b. Literature suggests that the drag co-efficient is a function of Re and sphericity or shape of the bubbles (Madhav & Chhabra, 1995), i.e.

$$C_d = f(\mathrm{Re}, \phi) \tag{12}$$

For the non-Newtonian power law fluids, the Re is estimated based on the apparent viscosity because the terminal velocity of the bubble changes with shear rate as the fluid viscosity is dependent on shear rate. The average shear rate over the entire bubble surface corresponds to U_b/d_w and the apparent viscosity is given (Dewsbury *et al,* 19990; Tsuge & Hibino, 1971) by:

$$\mu = K\left(U_b/d_w\right)^{n-1} \tag{13}$$

Here, *K* is the consistency index of the power law fluid.
Re for non-Newtonian power law fluid is rearranged into as follows [12, 17, 19, 25, 26].

$$Re = \frac{\rho_{liq}d_w^n U_b^{2-n}}{K} \tag{14}$$

NEW DRAG CORRELATION FOR NON-NEWTONIAN FLUIDS

At low Re, the shape of gas bubbles is close to spherical. Chhabra (2006) solved the governing equations for the creeping flow regime at low Re ($\mathrm{Re} \le 0.1$) which is a form of Stokes law. The Stokes model is given by,

$$C_d = \frac{24}{\mathrm{Re}} \tag{15}$$

At Re <0.1, the bubble velocity is dependant on the viscosity of the fluid and the gas bubble follows the Hadamard-Ryczynski model rather than the Stokes model due to the internal circulation of the gas bubble which is given (Miyahara & Yamanaka,1993) by,

$$C_d = \frac{16}{\mathrm{Re}} \tag{16}$$

Equations (15) and (16) are only valid for solid bubbles or particles at very low Re (< 0.1) and are not suitable for gas bubbles rising in power-law liquids at high Re.
For any Re, the following equation (17) was suggested for spherical bubbles (Mei & Klausner, 1992).

$$C_d = \frac{16}{\mathrm{Re}}\left\{1+\left[\frac{8}{\mathrm{Re}}+\frac{1}{2}\left(1+3.315\,\mathrm{Re}^{-0.5}\right)\right]^{-1}\right\} \tag{17}$$

The most widely accepted correlation of drag co-efficient for solid particles was developed by Turton & Levenspiel (1986) and is given by,

$$C_d = \frac{24}{\mathrm{Re}}\left(1+0.173\,\mathrm{Re}^{0.657}\right) + \frac{0.413}{1+16,300\,\mathrm{Re}^{-1.09}} \tag{18}$$

The above correlation converges to Stokes model at low Re number. A modified correlation proposed for gas bubbles in non-Newtonian power-law fluids, is given by,

$$C_d = \frac{16}{\mathrm{Re}}\left(1+0.173\,\mathrm{Re}^{0.657}\right) + \frac{0.413}{1+16,300\,\mathrm{Re}^{-1.09}} \tag{19}$$

Khan and Richardson (1987) also proposed correlations for bubble drag co-efficient at wide ranges of Re as follows,

$$C_d = \left[2.25\,\mathrm{Re}^{-0.31}+0.36\,\mathrm{Re}^{0.06}\right]^{3.45} \tag{20}$$

The above equation (20) is valid for (10^{-2}< Re <3*10^5).
Many authors have predicted the drag relationship which focused on either spherical bubbles or non spherical particles. After considering all these correlations above, it is evident that almost all correlations are formulated with the conventional relationship of C_d-Re where bubbles are considered spherical. It is known that bubbles are deformed in shape as their size increased. Shape instability is also a necessary phenomenon to be considered for the prediction of drag relationship. Therefore, a new correlation would need to be found in this study that is applicable to spherical and non spherical bubbles in non-Newtonian fluid crystal suspension. For this study, equation (21) was considered for the prediction of the spherical and non-spherical bubble in non-Newtonian fluids. It was modified by introducing the shape factor (ϕ) or flatness ratio of $\frac{d_w}{d_{eq}}$ into the original equation (19) as follows,

$$C_d = \frac{16}{\mathrm{Re}*\phi}*\left(1+0.173*\phi*\mathrm{Re}^{0.657}\right) + \frac{0.413}{1+16,300*\phi*\mathrm{Re}^{-1.09}} \quad (21)$$

The new correlation (equation 21) proposed in this study was compared with the experimental data and other published literature in this study.

EXPERIMENTAL FACILITY AND PROCEDURE

A schematic diagram of the experimental set-up is shown in Figure 1. The experimental rigs consisting of polycarbonate and acrylic tubes were constructed along with the bubble producing mechanism. The camera lifting apparatus for the video camera, the trigger mechanism; synchronization of the rise of the camera lifting device was fabricated. A high resolution Charge Coupled Device (CCD) video camera was used to capture video clips and still images during experimental program. Video clips and still images were analysed with commercial software to evaluate and analyse the bubble terminal velocity, size, shape and the drag force exerted on bubbles.

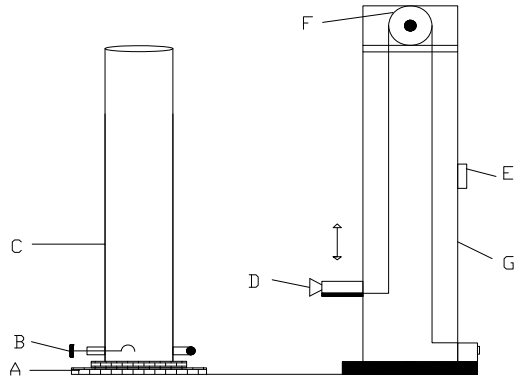

A = Sturdy Base; B = Rotating Spoon; C = Cylindrical test rig (0.125 m or 0.40 m diameter), D = Video camera; E = Variable speed motor; F = Pulley; and G = Camera lifting device.

Figure 1 Schematic diagram of experimental device

The details of the experimental apparatus and the experimental methods were described elsewhere [29, 30]. A known volume of air bubble was injected from injection apparatus close to the bottom of the test rig. The injection apparatus was designed in such a way that allows controllable quantities of air into the test rig. A CCD video camera recorded the bubble motion as they rose through liquids. These bubble videos clips were analysed by 'Windows Movie Maker' where various bubble rise times were noted. Bubble rise velocities over these times were calculated since the distance travelled was known.

Bubble equivalent diameter was computed from the still images which were obtained from the video clips. The still images were analysed using commercial software "SigmaScan Pro 5.0" and the bubble height (d_h) and the bubble width (d_w) were measured in pixels. The pixel measurements were converted to millimetres based on calibration data for the camera. The bubble equivalent diameter d_{eq} was calculated as an equivalent-sphere-volume.

MATERIALS

Three solutions were tested in this study. These included:

--a water solution;

--a non-Newtonian solution comprising of 0.05% concentration by weight of xanthan gum mixed with water; and

--a non-Newtonian crystal suspension comprising of 0.05% concentration by weight of xanthan gum mixed with water and 1% polystyrene crystal.

The rheological properties for the solutions were measured using an Advanced Rheometric Expansion System (ARES) with a bob and cup geometry (Hassan *et al,* 2007). The crystals used in this study were Dynoseeds TS 250 type, composed of 95-100% polystyrene. The crystals had a mean particle diameter of 0.23 mm and density of 1050 kg/m^3 allowing them to remain suspended and not settle in the xanthan gum solutions.

RESULTS AND DISCUSSION

The velocity of bubbles released in the three test solutions for bubble volumes of 0.1mL – 20.0mL at different liquid heights were presented in Figure 2.

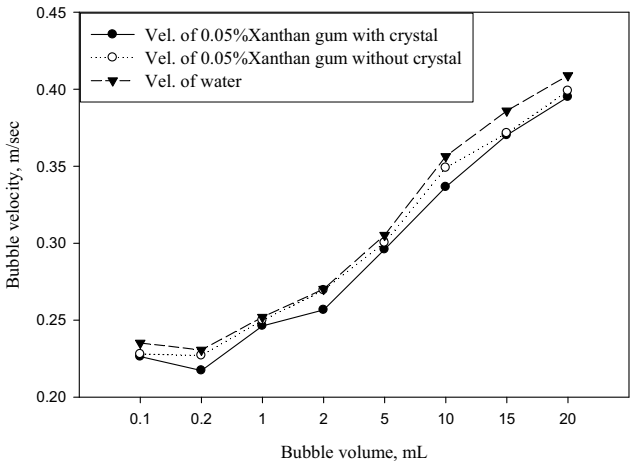

Figure 2 Comparison of bubble rise velocity for water, 0.05% xanthan gum and crystal suspension at 1 m height.

It is seen that the bubble velocity increases with an increase in bubble volume in all three liquids (water, 0.05% xanthan gum solution and xanthan gum crystal suspension). The average bubble velocity in 0.05% xanthan gum solution was observed less than that in water and the least in crystal suspension. This is due to the apparent increase in viscosity caused by the crystals in suspension. The higher viscosity restrains the bubble to rise faster.

The comparison of the values of Re with the bubble shape factors (ϕ) were illustrated in figure 3 and summarized in table 1. The Figure 3 shows that ϕ values increase as Re increases over the entire range investigated (35>Re<173).

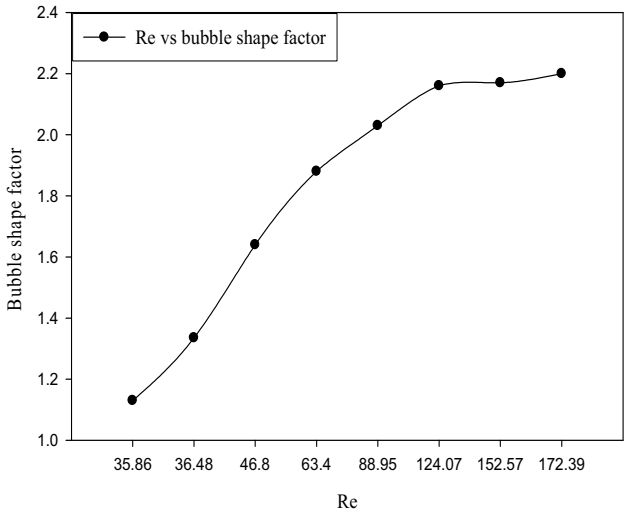

Figure 3 Comparison of the values of Re with bubble shape factor (ϕ).

Table 1 Re and shape factor (ϕ) values with respect to different bubble volumes.

Bubble volume, mL	Re	Shape factor, ϕ
0.1	35.86	1.13
0.2	36.48	1.335
1.0	46.80	1.64
2.0	88.95	1.88
5.0	63.40	2.03
10.0	124.07	2.16
15.0	152.57	2.17
20.0	172.39	2.20

Over the range (35>Re<124), ϕ increases uniformly and it remains nearly constant at a range of 124 <Re<172. For Re = 35.86 and ϕ = 1.13, the bubble has a nearly spherical shape.Experimental observations show that the bubbles change from spherical to ellipsoidal and ellipsoidal to spherical cap with the increase in bubble size and Re. These shape transitions were clearly observed (illustrated in Figure 4) at three different heights.

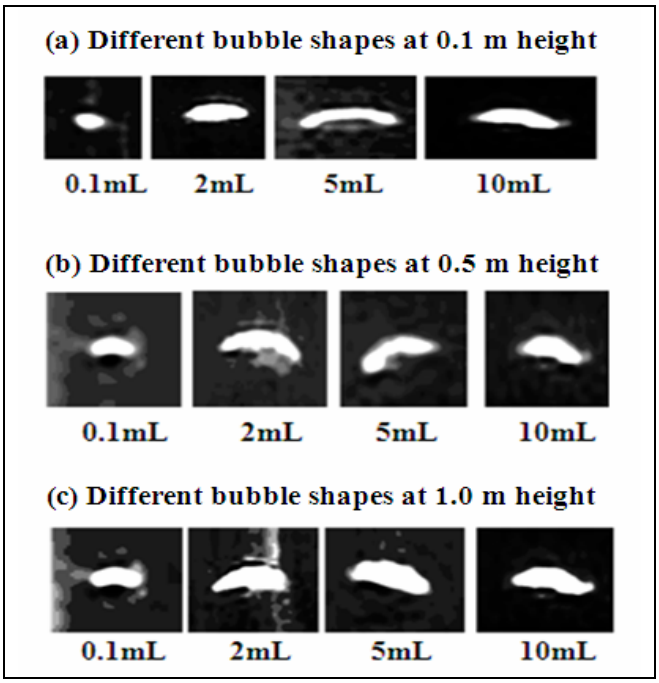

Figure 4 Different bubble shapes in crystal suspensions at three different heights.

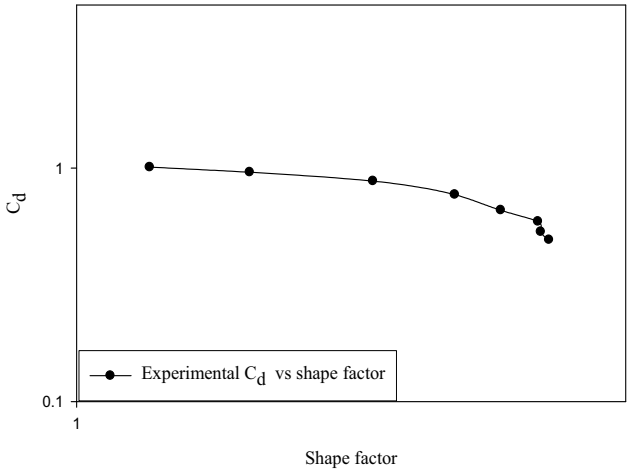

Figure 5 Experimental drag co-efficient versus bubble shape factor (ϕ)

Figure 4 shows that the bubbles encounter different shapes apart from the spherical, ellipsoidal and spherical-cap. The bubbles usually deform as their size increased and the rate of deformations were more pronounced at

higher values of ϕ and Re. Experimental drag coefficient as a function of ϕ was plotted in Figure 5. Observations from Figure 5 indicate that the drag coefficient decreases with increase in ϕ and the drag co-efficient data drop quickly at higher values of ϕ ($2<\phi<2.5$). This is due to the shape instability caused by the larger bubbles. As indicated from Figure 5, it can be evidenced that the bubble shape deformations have a great influence on drag co-efficient.

For the better prediction of the C_d-Re relationship, the addition of the shape factor with Re may be required to appropriately explain the effect of the shape of a bubble on the drag coefficient.

The bubble drag co-efficient, C_d as a function Re for the 0.05% xanthan gum crystal suspension was presented in Figure 6. As seen from Figure 6, the experimental drag co-efficient decreases uniformly over the entire range of Re investigated (35<Re<173). Figure 6 shows that the experimental C_d correlates reasonably well with some deviations observed initially when assessed with the widely accepted correlation of Dewsbury *et al.* (1999) proposed for non-Newtonian liquids. Correlations of Turton & Levenspiel (1986) and Khan & Richardson (1987) developed for spherical bubbles or particles in Newtonian liquids follow a similar but offset trend to the experimental data.

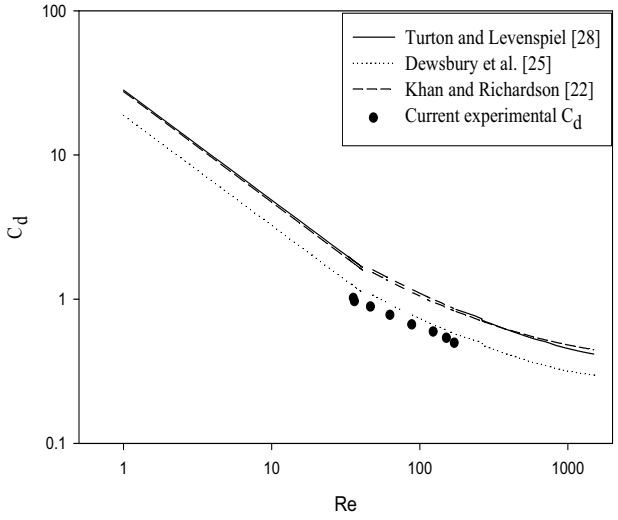

Figure 6 Drag co-efficient as a function of Reynolds number for rising air bubble in crystal suspended xanthan gum solution.

The new correlation (equation 21) was formulated in the ranges 0.1<Re<200 and $1<\phi<2.5$. Equation 21 differs from the correlation of Dewsbury *el al.* (1999) in that ϕ was introduced to characterize the flatness of the bubbles and the settling of non-spherical bubbles. The introduction of the shape factor also helps to elucidate the initial deviations of correlation of Dewsbury *el al.* (1999) to the experimental data. Equation (21) is compared with correlation of Dewsbury *el al.* (1999) in Figure 7. This new correlation was found to be consistent with this published correlation. Therefore, it can be concluded that this new correlation is applicable over the ranges, 0.1<Re<200 for both spherical and non-spherical air bubbles in power law non-Newtonian crystal suspensions.

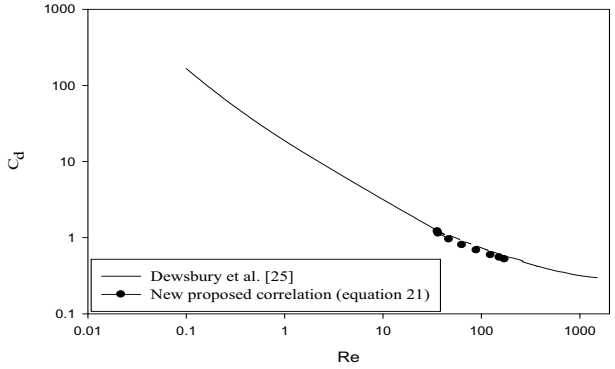

Figure 7 Drag co-efficient as a function of Reynolds number and shape factor for rising air bubble in crystal suspended xanthan gum solution.

CONCLUSION

Experimental measurements were conducted to analyze the characteristics of air bubbles of different sizes rising in non-Newtonian crystal suspensions. The bubble velocity and drag co-efficient data show an increase in velocity with the increase in bubble volume as the bubble rises through different liquids. The velocity results showed that the average bubble velocity was greater in water compared to crystal suspension mixtures. The lower velocity in crystal suspension mixtures is due to the increased viscosity of the crystal suspension resulting in higher friction on the surface which restricts the bubbles rising faster.

The relationship between C_d and Re for crystal suspended xanthan gum solution revealed acceptable results with slight deviations observed initially when compared with appropriate C_d predictions found in the literature. A new drag correlation as a function of Re and the bubble shape factor was proposed for the prediction of the drag co-efficient of spherical and non-spherical bubbles to rectify this deviation. This new correlation produced consistent results with the experimental drag co-efficient and the published literature. It can be concluded that this new correlation could be applicable

for air bubbles in both Newtonian and non-Newtonian fluids over the range 0.1 <Re < 200.

ACKNOWLEDGEMENT

The authors gratefully acknowledges the financial support from Sugar Research Institute, Queensland, Australia and the technical assistance provided by Mr. Ray Kearney in the experimental works. N.M.S. Hassan is thankful to CQUniversity and PELM for the award of a research scholarship to pursue this study.

NOMENCLATURE

d_h [m] bubble height

d_w [m] bubble width or projected diameter on to horizontal plane

d_{eq} [m] bubble equivalent diameter

A_V [m^3] surface of a sphere having same volume as the bubble

A [m^2] projected bubble surface area

Re [-] Reynolds number

c_d [-] drag co-efficient

F_d [N] drag force

F_G [N] gravity force

F_B [N] buoyancy force

g [m/s^2] acceleration due to gravity

U_b [m/s] bubble rise velocity

n [-] power law index

K [$Pa.s^n$] consistency index of the power law fluid

g [m/s^2] gravitational acceleration

V [m] bubble volume

$\frac{d_w}{d_{eq}}$ [-] bubble flatness ratio

K_1 [-] arbitrary constant

Greek letters

$\Delta\rho$ [kg/m^3] density difference between liquid and air bubble

ρ_{liq} [kg/m^3] liquid density

μ [Pa.s] apparent viscosity

$\dot{\gamma}$ [1/s] shear rate

ϕ [-] shape factor

REFERENCES

Chhabra, R. P. 1993. Bubbles, Drops and Particles in Non-Newtonian Fluids, Boca Raton, FL

Chhabra, R. P., Richardson, J. F. 1999. Non-Newtonian flow in the process industries, Butterworth-Heinemann, Oxford

Chhabra, R. P. 1990. Motion of spheres in power law (viscoelastic) fluids at intermediate Reynolds numbers, a unified approach, Chem. Eng. Process, 28, pp. 89–94.

Chhabra, R. P. 2006. Bubbles, Drops and Particles in Non-Newtonian Fluids, second edition, Boca Raton, FL

Clift, R., Grace, J. R., Weber, M. E. 2005. Bubbles, drops and particles; Academic Press, 1978, republished by Dover

Dalton, D. S. 1967. A drag coefficient correlation for spheres settling in Ellis fluids, PhD Thesis, University of Utah, Salt Lake City, UT

Dewsbury, K., Karamanev, D. G., Margaritis, A. 1999. Hydrodynamic characteristics of free rise of light solid particles and gas bubbles in non-Newtonian liquids, Chem. Eng. Sci., 54, pp. 4825-4830.

Dewsbury, K., Karamanev, D. G., Margaritis, A. 2000. Dynamic behaviour of freely rising buoyant solid spheres in non-Newtonian liquids, AIChE J., 46 (1)

Dewsbury, K., Karamanev, D. G., Margaritis, A. 2002. Rising solid sphere hydrodynamics at high Reynolds numbers in non-Newtonian fluids, Chem. Eng. J., 87, pp. 129-133.

Dhole, S. D., Chhabra, R. P., Eswaran, V. 2007. Drag of a spherical bubble rising in power law fluids at intermediate Reynolds numbers, Ind. Eng. Chem. Res., 46, pp. 939-946.

Gabito, J., Tsouris, C. 2008. Drag coefficient and settling velocity for particles of cylindrical shape, Powder Technology, 183, pp. 314-322.

Haider, A. M., Levenspiel, O. 1989. Drag coefficient and terminal velocity of spherical and non-spherical particles, Powder Technocol, 58, pp. 63-70

Hassan, N. M. S., Khan, M. M. K., Rasul, M. G., Rackemann, D. W. 2007. An experimental study of bubble rise characteristics in non-Newtonian fluids, Proceedings of the 16th Australasian Fluid Mechanics Conference, Gold Coast, Australia, pp. 1315-1320.

Karamanev, D. 1994. Rise of gas bubbles in quiescent liquids, AIChE J. 40, pp. 1418-1421.

Kelessidis, V. C. 2004. Terminal velocity of solid spheres falling in Newtonian and non-Newtonian liquids, Chem. Eng. Sci., 59, pp. 4437-4447.

Khan, A. R., Richardson, J. F. 1987. The resistance to motion of a solid sphere in a fluid, Chem. Eng. Commun., 62, pp. 135-150.

Lali, A. M., Khare, A. S., Joshi, J. B., Nigam, K. D. P. 1989. Behaviour of solid particles in viscous non-Newtonian solutions: settling velocity, wall effects and bed expansion in solid-liquid fluidized beds, Powder Technology, 57, pp. 39.

Margaritis, A., Bokkel, D. W., Karamanev, D. G. 1999. Bubble rise velocities and drag co-efficients in non-Newtonian polysaccharide solutions, John Wiley & Sons, Inc.

Mei, R., Klausner, J. F. 1992. Unsteady force on a spherical bubble at finite Re with small functions in the free stream velocity, Phys. Fluids A, 4

Miyahara, T., Yamanaka, S. 1993. Mechanics of motion and deformation of a single bubble rising through quiescent highly viscous Newtonian and non-Newtonian media, J. Chem. Eng., Japan, 26

Prakash, S. 1983. Experimental evaluation of terminal velocity in non-Newtonian fluids in the turbulent region, Chem. Eng., 25, pp. 1-4

Shah, S. N., Fadili, Y. El., Chhabra, R. P. 2007. New model for single spherical particle settling velocity in power law (visco-inelastic) fluids, Int. J. Multiphase Flow, 33, pp. 51-66.

Thompson, T. L., Clark, N. N. 1991. Powder Technocol, 67, pp. 57

Trang-Cong, S., Gay, M., Michaelides, E. E. 2004. Drag coefficients of irregularly shaped particles, Powder Technocol, 139, pp. 21 -32

Tsuge, H., Hibino, S. 1971. The motion of single gas bubbles rising in various liquids, Kagaku Kogaku, 35

Turton, R., Levenspiel, O. 1986. A short note on the drag correlation for spheres, Powder Technology, 4

Unnikrishan, A., Chhabra, R. P. 1991. An experimental study of motion of cylinders in Newtonian fluids: wall effects and drag coefficient, Can. J. Chem. Eng., 69, pp. 729-735.

Venu Madhav, G., Chhabra, R. P. 1995. Drag on non-spherical particles in viscous fluids, Int. J. Miner. Process, 43, pp. 15-29

Wadel, H. 1933. Sphericity and roundness of rock particles, J. Geol., 41, pp. 310-331.